

Dehydration of D-xylose into furfural over H-zeolites

Saet Byul Kim*, Su Jin You*, Yong Tae Kim*, SangMin Lee**, Hyokyu Lee**, Kihyun Park**, and Eun Duck Park**†

*Division of Energy Systems Research and Division of Chemical Engineering and Materials Engineering,
Ajou University, Wonchun-dong, Yeongtong-gu, Suwon 443-749, Korea

**R&D Center Kolon Industries, Inc., 294 Gajwa-dong, Seo-gu, Incheon 404-250, Korea

(Received 2 July 2010 • accepted 30 August 2010)

Abstract—The liquid-phase dehydration of D-xylose into furfural was carried out over various H-zeolites-H-ferrierite, H- β , H-ZSM-5, H-Y and H-mordenite-with various SiO₂/Al₂O₃ molar ratios in different solvent systems: water, dimethyl sulfoxide (DMSO) and a mixture of water and toluene (water/toluene). For comparison, γ -Al₂O₃ and silica-alumina were also examined. FT-IR spectroscopy after pyridine adsorption was conducted to probe the acidity of the H-zeolites. The D-xylose conversion and furfural yield generally decreased with increasing SiO₂/Al₂O₃ molar ratio over the H-zeolites having the same crystal structure irrespective of the kind of solvent system. This is closely related to the accessible acid sites. In a comparison study using the three different solvent systems, the D-xylose conversion and furfural selectivity generally decreased in the following order: water/toluene>DMSO>water. In water and water/toluene, H- β (25) showed the highest furfural selectivity at a similar D-xylose conversion among the tested zeolites. On the other hand, H-mordenite (20) showed the highest furfural selectivity at a similar D-xylose conversion in DMSO.

Key words: Dehydration, D-xylose, Furfural, Zeolite, Acidity

INTRODUCTION

The need for environmentally benign chemical processes to substitute for fossil-based chemical processes has recently arisen because of the limited reservoir of fossil resources and the increasing attention being given to environmental issues. Carbohydrates are by far the most abundant organic compounds on earth and represent the major portion of the annually renewable biomass of about 200 billion tons [1]. These abundant renewable carbohydrates (glucose, fructose and xylose) can be easily converted into monosaccharides. Because of their plentiful CHO-containing structure, the production of chemicals using processes based on monosaccharides can compete with petroleum-based processes.

Among the various industrial chemical products, furfural (C₅H₄O₂) is one of the key renewable ones because of its wide range of industrial applications for the production of various chemical products (nylon, lubricants, solvents, adhesives, medicine and plastics). It can be produced from hemicelluloses by the dehydration of pentosans such as xylose whose hydroxyl groups can be selectively eliminated under aqueous acidic condition [2].

Since the 1920s, furfural has been produced from agricultural organic residues in industrial plants. To improve the selectivity to furfural, various mineral acids such as sulfuric acid [2-8], hydrochloric acid [6,7], trifluoroacetic acid [7], nitric acid [7] and phosphoric acid [7,9], were introduced. Although concentrated mineral acids can maximize the yield of furfural, it is difficult to handle these homogeneous catalysts in industrial processes because of their high toxicity and corrosiveness. Excessive amounts of water also have to be used to neutralize the mineral acid, resulting in the formation

of a large quantity of wastewater.

To overcome the drawbacks of these mineral acids, various homogeneous and heterogeneous catalysts have been suggested for the production of furfural [10-21], including 1-alkyl-3-methylimidazolium ionic liquids [10] and keggin-type heteropolyacids [11]. Compared with homogeneous catalysts, heterogeneous catalysts can be considered to be more plausible, because of the advantages they afford in terms of separation and safety. Various solid acid catalysts such as non-soluble heteropolyacids (C_sH_{3-x}PW₁₂O₄₀) [12], mesoporous silica-supported 12-tungstophosphoric acid [13], sulfated zirconia [14], sulfonic acid functionalized MCM-41 [15], niobium silicates [16], layered metal oxides (titanates, niobates, and titanoniobates) [17], zeolites [18-20] and silicoaluminophosphates (SAPOs) [21] were examined.

It is considered that both the structural properties and acidity affects the activity of a heterogeneous catalytic system for the dehydration of D-xylose. Zeolites are adequate solid acid catalysts because of their tunable acidity and shape selectivity. When H-mordenite (SiO₂/Al₂O₃=5.5) with a low mesoporous volume were used as catalysts in water/toluene, a higher selectivity for furfural was obtained as compared with H-faujasite (SiO₂/Al₂O₃=7.5) because of their shape selectivity [18]. Lima et al. studied the improvement of the diffusion limitation using zeolites for the dehydration of D-xylose and showed that the dealuminated zeolites, obtained from layered aluminosilicate Nu-6 (SiO₂/Al₂O₃~14.5), gave a higher furfural yield than H-mordenite (SiO₂/Al₂O₃~2.5) for the production of furfural in water/toluene [19]. Proton type zeolites such as H-ZSM-5 (SiO₂/Al₂O₃=14) were also used as catalysts to estimate the reaction mechanism and the kinetics parameters [20]. However, no relevant work for variations such as SiO₂/Al₂O₃ molar ratio and structure of H-zeolite was performed over various H-zeolites.

We investigated the catalytic activity of various zeolites, viz. H-

†To whom correspondence should be addressed.

E-mail: edpark@ajou.ac.kr

mordenite, H-ZSM-5, H-ferrierite, H-Y and H- β with different SiO₂/Al₂O₃ molar ratios for the liquid-phase dehydration of D-xylose into furfural in different solvent systems: DMSO, water and water/toluene. To compare with H-zeolites, γ -Al₂O₃ and amorphous silica-alumina were also examined.

EXPERIMENTAL

1. Catalysts

We purchased various solid acid catalysts: H-ferrierite (SiO₂/Al₂O₃=20, Zeolyst, CP914C, S_{BET}=389.9 m²/g), H-ferrierite (SiO₂/Al₂O₃=55, Zeolyst, CP914, S_{BET}=381.6 m²/g), H- β (SiO₂/Al₂O₃=25, Zeolyst, CP814E, S_{BET}=508.1 m²/g), H- β (SiO₂/Al₂O₃=27, Tosoh, HSZ-930 NHA, S_{BET}=597.5 m²/g), H- β (SiO₂/Al₂O₃=38, Zeolyst, CP814C, S_{BET}=578.3 m²/g), H- β (SiO₂/Al₂O₃=350, Zeolyst, CP811C-300, S_{BET}=698.8 m²/g), NH₄-ZSM-5 (SiO₂/Al₂O₃=23, Zeolyst, CBV2314, S_{BET}=572.4 m²/g), H-ZSM-5 (SiO₂/Al₂O₃=30, Zeolyst, CBV3014E, S_{BET}=364.0 m²/g), H-ZSM-5 (SiO₂/Al₂O₃=60, Süd-Chemie, S_{BET}=487.1 m²/g), H-ZSM-5 (SiO₂/Al₂O₃=150, Süd-Chemie, S_{BET}=460.4 m²/g), H-ZSM-5 (SiO₂/Al₂O₃=500, Zeocat, S_{BET}=383.1 m²/g), H-ZSM-5 (SiO₂/Al₂O₃=1000, Zeocat, S_{BET}=311.8 m²/g), H-Y (SiO₂/Al₂O₃=5.1, Zeolyst, CBV400, S_{BET}=631.4 m²/g), NH₄-mordenite (SiO₂/Al₂O₃=20, Zeolyst, CBV21A, S_{BET}=423.8 m²/g), γ -Al₂O₃ (Strem Chem., S_{BET}=212.9 m²/g) and silica-alumina (SiO₂/Al₂O₃=6.6, Aldrich, S_{BET}=572.0 m²/g). All of the zeolites were pretreated in air at 600 °C before the reaction. To differentiate the various catalysts, their SiO₂/Al₂O₃ molar ratios are presented in parentheses.

2. Characterization of Catalysts

The BET surface area was calculated from the N₂ adsorption data that were obtained with an Autosorb-1 apparatus (Quantachrome) at a liquid N₂ temperature. Before the measurement, the sample was degassed in a vacuum for 4 h at 200 °C.

A self-supporting wafer consisting of 20 mg of each sample was placed in an *in situ* IR cell with CaF₂ window and connected to a vacuum system. The wafer was dehydrated at 250 °C and P<10⁻⁷ bar for 1 h. The background spectra of the samples were recorded after the self-supported wafer was cooled to room temperature and pyridine vapors were admitted to the cell at room temperature for 30 min. The samples were cooled to room temperature after evacuation for 1 h at a temperature (150 and 250 °C) and the spectra were recorded on a NICOLET 6700 spectrometer with a resolution of 4.0 cm⁻¹.

3. Catalytic Activity Tests

D-xylose was dehydrated into furfural in a batch reactor. 0.20 M D-xylose (Sigma-Aldrich, 99%) and the catalyst were mixed with 30 ml of solvent, and the resulting mixture was introduced into an autoclave. When a mixture of water/toluene, which is simply denoted as W/T, was used as the solvent, the volumetric ratio of water to toluene was fixed at 3 : 7. The reactor was filled with nitrogen for 10 min. The slurry was stirred with a magnetic stirrer at 500 rpm. After the reaction, the autoclave was cooled to room temperature and the products were filtered with a 0.2 μ m membrane filter and analyzed with a high performance liquid chromatograph (Waters, 1525 Binary HPLC Pumps) equipped with a 2487 dual-wavelength absorbance detector (Waters) at 280 nm for furfural and refractometer detector (Waters) for D-xylose and lyxose. To separate the D-xylose and lyxose in the aqueous-phase, an H⁺-form ion exchange

column (PL Hi-Plex H 300 \times 7.7, Varian) with 0.01 M H₂SO₄ solutions was utilized. Products such as furfural in the organic phase were separated with an ODS column (Spherisorb ODS S10C18 250 \times 4.6, Waters) with 40 vol% CH₃OH solution.

The D-xylose conversion and molar carbon selectivity for the products such as furfural and lyxose were calculated based on the following formula:

$$\text{D-xylose conversion } (X_{D\text{-xylose}}) = \frac{C_{D\text{-xylose, in}} - C_{D\text{-xylose, out}}}{C_{D\text{-xylose, in}}}$$

$$\text{Molar carbon selectivity } (S_{\text{Product}}) = \frac{C_{\text{Product}}}{C_{D\text{-xylose, in}} - C_{D\text{-xylose, out}}}$$

where $C_{D\text{-xylose, in}}$ is the initial molar concentration of D-xylose, $C_{D\text{-xylose, out}}$ is the molar concentration of D-xylose after the reaction, and C_{Product} is the molar concentration of the products such as furfural and lyxose after the reaction.

RESULTS AND DISCUSSION

The surface acidity is an important factor for the dehydration of D-xylose into furfural, because this reaction can occur on the surface acid sites of the solid catalysts. FT-IR spectroscopy was employed to analyze the surface acidity of the various solid acid catalysts such as H-zeolites, γ -Al₂O₃ and silica-alumina. Fig. 1 shows the IR spectra of the solid acid catalysts after desorbing pyridine, which was already adsorbed on the solids at RT, in vacuum at 150 and 250 °C. In the FT-IR spectra after pyridine adsorption, the bands of pyridine protonated by Brønsted acid sites (pyridinium ions, PyH⁺) appear at \sim 1,540 and 1,640 cm⁻¹, while the bands from pyridine coordinated to Lewis acid sites (coordinatively unsaturated Al³⁺, PyL) appear at \sim 1,454 and 1,622 cm⁻¹ [22]. In addition, the band at 1,490 cm⁻¹ may result from the combination of the Brønsted and Lewis adsorbed species [23]. For the solid acid catalysts tested in this work, the two distinct new bands at 1,445 and 1,596 cm⁻¹ appeared. These bands are due to the pyridine adsorbed on H-bond donor sites (the surface OH groups, HPy) interacting through hydrogen bond [24]. Both H- β (350) and H-ZSM-5 (500) after degassing the chemisorbed pyridine at 150 °C exhibited the same adsorption bands at 1,437 and 1,580 cm⁻¹ corresponding to the physisorbed pyridine (PPy) in the literature [24]. These bands disappeared when the desorption temperature increased up to 250 °C. The strong Lewis acid sites and a weak H-bond donor sites were observed over γ -Al₂O₃. In the case of H- β , H-ZSM-5 and H-ferrierite, the intensity of the bands at 1,445 and 1,548 cm⁻¹ representing the H-bonded donor sites and Brønsted acid sites decreased with increasing SiO₂/Al₂O₃ molar ratio, which was in good agreement of the NH₃-TPD results in the literature [25]. As shown in Fig. 1, the intensity of the band at 1,445 cm⁻¹ representing to H-bond donor sites decreased with increasing the pyridine desorption temperature, whereas the intensity of the band at 1,454 and 1,548 cm⁻¹ representing to Lewis acid sites and Brønsted acid sites did not change noticeably. The decrease of the weakly adsorption bands of Lewis acid sites as well as those of H-bonded donor sites with increasing desorption temperature can be interpreted that these adsorption sites are due to the presence of the octahedral Al³⁺ sites [24]. On the other hand, the Lewis acid sites remaining even after degassing at 250 °C is due to the presence of the tetrahedral Al⁴⁺ sites [24]. These FT-IR spectra in

combination with NH_3 -TPD results [25,26] support that the weaker acid sites in the low-temperature (LT) region at temperatures below 300 °C in the NH_3 -TPD pattern could correspond to the Lewis acid sites. Since the intensity of the IR band is linearly related to the acid

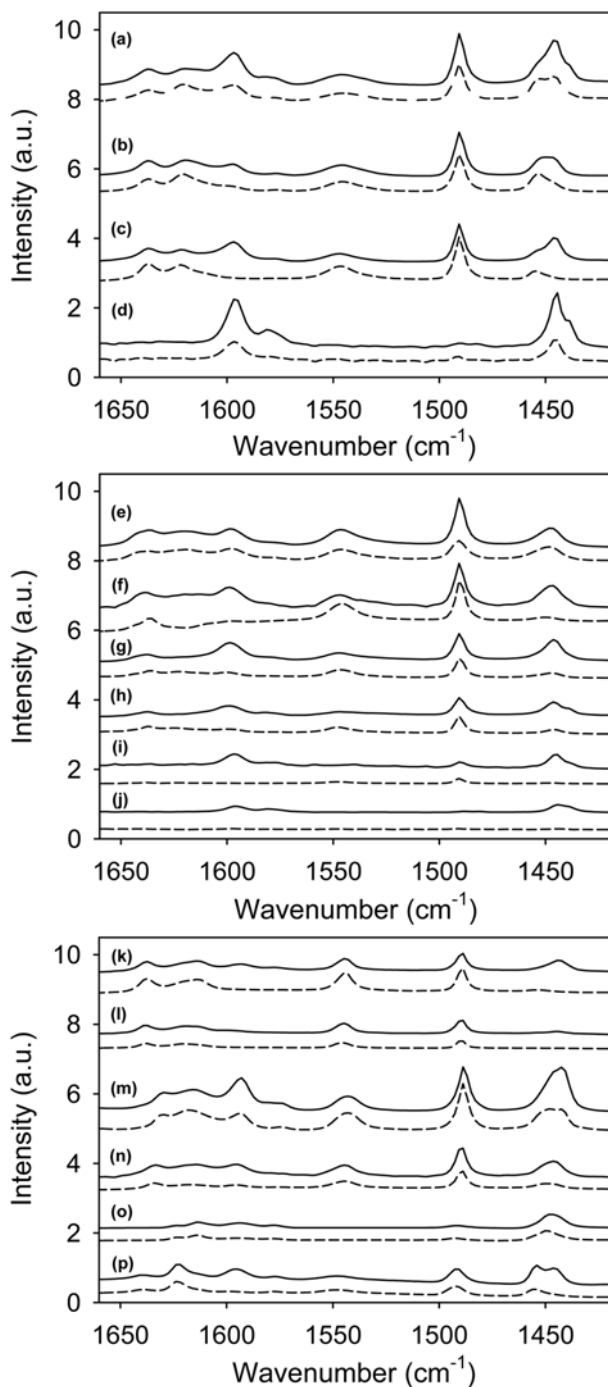


Fig. 1. FT-IR spectroscopic spectra after desorbing pyridine, which was already adsorbed on the catalyst at RT, in vacuum at 150 °C (solid line) and 250 °C (dotted line) for the solid acid catalysts, viz. H- β (25) (a), H- β (27) (b), H- β (38) (c), H- β (350) (d), H-ZSM-5 (23) (e), H-ZSM-5 (30) (f), H-ZSM-5 (60) (g), H-ZSM-5 (150) (h), H-ZSM-5 (500) (i), H-ZSM-5 (1000) (j), H-ferrierite (20) (k), H-ferrierite (55) (l), H-Y (5.1) (m), H-mordenite (n), γ - Al_2O_3 (o) and silica-alumina (p).

site concentration [27], the relative amount of the strong surface acid sites remaining after degassing at 250 °C can be estimated over solid acid catalysts at the similar total amount of acid sites obtained by NH_3 -TPD [25]. The amount of Brønsted acid sites decreased in the following order: H- β (25) > H-ZSM-5 (23) > H-Y (5.1) > H-ferrierite (20) > silica-alumina > H-mordenite (20) > γ - Al_2O_3 . The amount of Lewis acid sites decreased in the following order: H- β (25) > γ - Al_2O_3 > H-mordenite (20) > H-Y (5.1) > silica-alumina > H-ferrierite (20) > H-ZSM-5 (23). The total amount of acid sites decreased in the following order: H- β (25) > H-ZSM-5 (23) > H-Y (5.1) > H-ferrierite (20) > H-mordenite (20) > silica-alumina > γ - Al_2O_3 .

We used three different solvent systems: water, dimethyl sulfoxide (DMSO) and water/toluene. Liquid water is a well-known solvent having polar and protic properties. It can form H^+ ions capable of promoting the dehydration reaction at temperatures near 200 °C under near critical conditions [28,29]. DMSO, which is a polar and aprotic solvent, has a large dielectric constant and a similar lattice structure to water. To improve the selectivity for furfural, toluene can be used as an organic layer to extract the organic products from the aqueous phase. As presented in Table 1, noticeable catalytic activity was obtained over all of the catalysts in water, DMSO and water/toluene. The catalytic activity, as indicated by the D-xylose conver-

Table 1. The catalytic activity for the dehydration of D-xylose over the various solid acid catalysts in different solvent systems^a

Entry	Solvent	Catalysts	D-xylose conversion (%)	Furfural selectivity (%)	Furfural yield (%)
1	Water	-	22.1	23.0	5.1
2		H-ferrierite (20)	44.6	28.9	12.9
3		H- β (25)	51.5	36.9	19.0
4		H-ZSM-5 (23)	56.8	30.2	17.2
5		H-Y (5.1)	70.8	31.0	21.9
6		H-mordenite (20)	40.0	30.4	12.2
7		γ - Al_2O_3	84.2	24.5	20.6
8		Silica-alumina	42.9	35.6	15.3
9	DMSO	-	37.5	4.6	1.7
10		H-ferrierite (20)	74.1	31.3	23.2
11		H- β (25)	89.7	26.7	23.9
12		H-ZSM-5 (23)	69.3	29.6	20.5
13		H-Y (5.1)	61.1	1.6	1.0
14		H-mordenite (20)	61.9	38.7	24.0
15		γ - Al_2O_3	85.0	14.8	12.6
16		Silica-alumina	90.7	11.8	10.7
17	W/T	-	28.1	8.0	2.2
18		H-ferrierite (20)	79.6	44.3	35.3
19		H- β (25)	89.5	44.5	39.8
20		H-ZSM-5 (23)	89.7	47.7	42.8
21		H-Y (5.1)	97.4	42.2	41.1
22		H-mordenite (20)	81.1	43.4	35.2
23		γ - Al_2O_3	98.6	30.9	30.5
24		Silica-alumina	99.3	41.4	41.1

^aReaction conditions: D-xylose concentration=0.20 M, volume of solvent (Water, DMSO, and Water/toluene (3 : 7 by volume))=30 ml; Catalyst weight=0.30 g; reaction temperature=140 °C, reaction time=4 h

sion and furfural yield, was dependent on the kind of solvent in the reaction system and generally decreased in the following order: water/toluene>DMSO>water. In water, a strong interaction between the

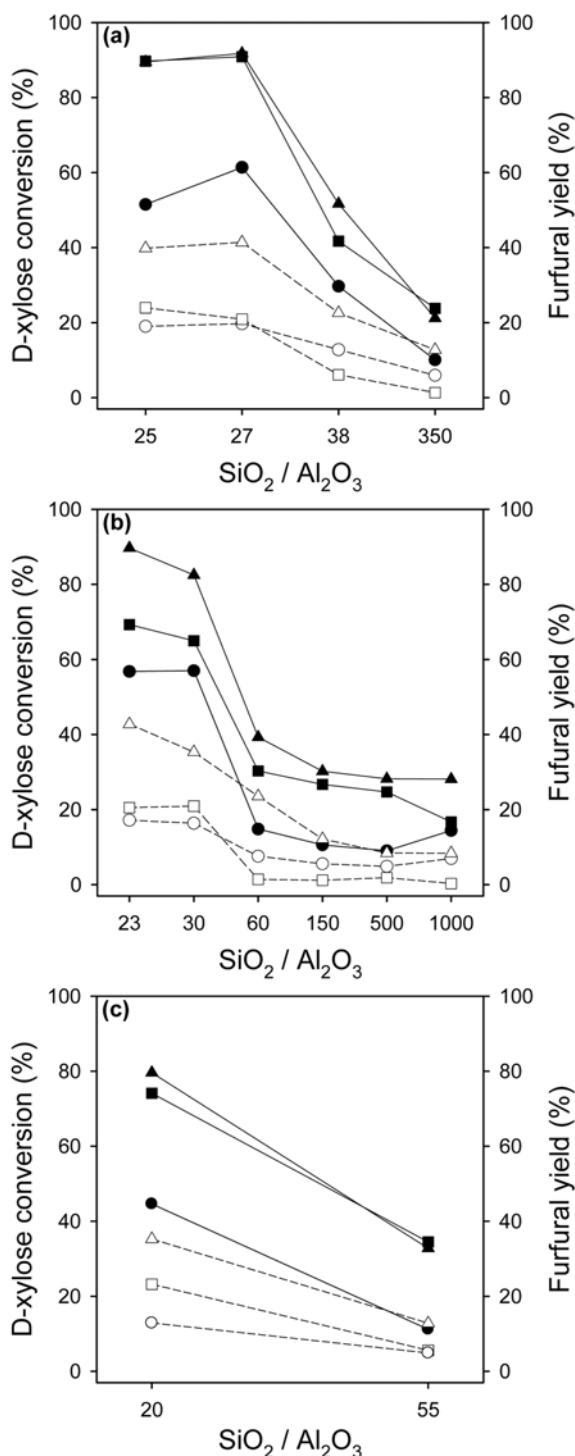


Fig. 2. D-xylose conversion (filled points) and furfural yield (unfilled points) over various H-zeolites, viz. H- β (a), H-ZSM-5 (b) and H-ferrierite (c) with a different $\text{SiO}_2/\text{Al}_2\text{O}_3$ molar ratio. Reaction conditions: D-xylose concentration=0.20 M, Catalyst weight=0.30 g, volume of solvent (water (●), DMSO (■) and water/toluene (v/v=3 : 7) (▲))=30 ml; reaction temperature=140 °C, reaction time=4 h.

polar solvent and the hydrophilic surface of the catalyst exists and water can block and/or poison the surface acidic sites. This might cause the lowest catalytic activity in water. Compared with the case where water was used as the solvent, the catalytic activity was significantly improved when toluene was used as the extraction solvent, suggesting that the organic products adsorbed on the catalysts can block the active sites for the conversion of D-xylose in water. This is identical to the previous reports that toluene is suitable as an organic extraction solvent to separate the organic products from the aqueous phase [30].

We also conducted the dehydration of D-xylose in the absence of a catalyst. As shown in Table 1 (entries 1, 9, and 17), the D-xylose conversion was dependent on the kind of solvent and decreased in the following order: DMSO>water/toluene>water. Indeed, slight activity (D-xylose conversion=22.1%) was observed in water, even in the absence of an acid catalyst. These results support the hypothesis that spontaneous D-xylose dehydration can occur in the absence of a catalyst and may be affected by the kind of solvent. It is worth noting that the furfural selectivity is quite low in the absence of a solid acid catalyst in DMSO due to its aprotic property acting as a hydrogen-bond donor [30]. The catalytic activity for the liquid-phase dehydration of D-xylose into furfural was examined over H-ferrierite, H-ZSM-5 and H- β with different $\text{SiO}_2/\text{Al}_2\text{O}_3$ molar ratios in water, DMSO and water/toluene, as shown in Fig. 2. In all of the solvent systems, the D-xylose conversion and furfural yield generally increased with decreasing $\text{SiO}_2/\text{Al}_2\text{O}_3$ molar ratio.

As revealed by FT-IR spectra after pyridine adsorption, the surface acidic properties, such as the acid strength, acid types and surface acid concentration, are dependent on the crystal structure and $\text{SiO}_2/\text{Al}_2\text{O}_3$ molar ratio. Various elementary reactions from D-xylose can take place over acid sites in the catalysts. A good correlation can be observed between the catalytic activity at 140 °C and the total amount of acid sites for the catalysts with the same crystal structure. This is in accordance with the results of Dias et al. [17], in which the initial catalytic activity (TOF) generally increased linearly with increasing total amount of acid sites (Brønsted acid sites and Lewis acid sites) measured by the IR spectroscopy of adsorbed pyridine over the exfoliated-aggregated nanosheet solid acid catalysts.

To investigate the effect of the crystal structure, a comparative study was conducted over the solid acid catalysts, which have a similar $\text{SiO}_2/\text{Al}_2\text{O}_3$ molar ratio, in water, DMSO and water/toluene, as listed in Table 1. $\gamma\text{-Al}_2\text{O}_3$ and silica-alumina also examined for comparison. In water, the D-xylose conversion decreased in the following order: $\gamma\text{-Al}_2\text{O}_3$ >H-Y (5.1)>H-ZSM-5 (23)>H- β (25)>H-ferrierite (20)>silica-alumina>H-mordenite (20), while the furfural yield decreased in the following order: H-Y (5.1) $\geq\gamma\text{-Al}_2\text{O}_3\geq\text{H-}\beta$ (25)>H-ZSM-5 (23)>silica-alumina>H-ferrierite (20) $\geq\text{H-mordenite}$ (20). In water/toluene, the D-xylose conversion decreased in the following order: silica-alumina $\geq\gamma\text{-Al}_2\text{O}_3\geq\text{H-Y}$ (5.1)>H-ZSM-5 (23) $\geq\text{H-}\beta$ (25)>H-mordenite (20)>H-ferrierite (20), while the furfural yield decreased in the following order: H-ZSM-5 (23) $\geq\text{H-Y}$ (5.1) $\sim\text{silica-alumina}\geq\text{H-}\beta$ (25)>H-ferrierite (20) $\geq\text{H-mordenite}$ (20) $\geq\gamma\text{-Al}_2\text{O}_3$. For comparison, the reaction was conducted under the same reaction condition with those in Table 1 except that 0.15 mmol of H_2SO_4 was used instead of the solid acid catalysts. In water/toluene, the D-xylose conversion and furfural selectivity was 45.8 and 47.6%, respectively. The D-xylose conversion was lower in the presence of homoge-

neous H₂SO₄ catalyst compared with the cases with the solid acid catalysts, whereas the furfural selectivity obtained in the homogeneous H₂SO₄ catalyst was similar to those obtained in the active solid acid catalysts. In DMSO, the D-xylose conversion decreased in the following order: silica-alumina \geq H- β (25) $>$ γ -Al₂O₃ $>$ H-ferrierite (20) $>$ H-ZSM-5 (23) $>$ H-mordenite (20) \geq H-Y (5.1), while the furfural yield decreased in the following order: H-mordenite (20) \geq H- β (25) \geq H-ferrierite (20) $>$ H-ZSM-5 (23) $>$ γ -Al₂O₃ $>$ silica-alumina $>$ H-Y (5.1).

γ -Al₂O₃ having only Lewis acid sites exhibited the high D-xylose conversion, while showing low furfural selectivity.

To clarify the effect of the crystal structure of the zeolites on the furfural selectivity, the furfural selectivity was compared over zeolites which have similar total amounts of acid sites at a similar D-xylose conversion, as shown in Table 2. In water, the furfural selectivity at a similar D-xylose conversion decreased in the following order: H- β (25) $>$ H-Y (5.1) \geq H-ZSM-5 (23) $>$ silica-alumina-H-mordenite (20) $>$ H-ferrierite (20) $>$ γ -Al₂O₃. In water/toluene, the furfural selectivity at a similar D-xylose conversion decreased in the following order: H- β (25) $>$ H-ferrierite (20) \geq H-ZSM-5 (23)-H-mordenite (20) \sim silica-alumina \geq H-Y (5.1) $>$ γ -Al₂O₃. In DMSO, the furfural selectivity at a similar D-xylose conversion decreased in the following order: H-mordenite (20) $>$ H-ZSM-5 (23) $>$ H-ferrierite (20) $>$ H- β (25) $>$ γ -Al₂O₃ $>$ silica-alumina $>$ H-Y (5.1). In water and water/toluene, H- β (25) showed the highest furfural selectivity among the tested

solid acid catalysts. In DMSO, H-mordenite (20) showed the highest furfural selectivity among the tested solid acid catalysts. It is worth mentioning that the strong Brønsted acid sites are beneficial for the high furfural selectivity in water and water/toluene.

Moreau et al. suggested that H-modernite (6.5 \times 7.0 Å \leftrightarrow 2.6 \times 5.7 Å, bidimensional structure) is more selective than H-Y (7.4 \times 7.4 Å, tridimensional structure) at 170 °C in water/toluene (1 : 3 by volume), because H-Y has large cavities with a size of about 13 Å which allows side reactions to occur, such as the rearrangement of furfural and/or degradation [18]. From this view point, it is reasonable that H-ferrierite (4.2 \times 5.4 Å \leftrightarrow 3.5 \times 4.6 Å, bidimensional structure) and H-ZSM-5 (5.1 \times 5.5 Å \leftrightarrow 5.3 \times 5.6 Å, tridimensional structure) showed similar furfural selectivities to H-mordenite. Among them, H- β (6.6 \times 6.7 Å \leftrightarrow 5.1 \times 5.6 Å, tridimensional structure) can be chosen as the most selective catalyst because of its optimum channel size.

DMSO has been applied to dehydration reactions to increase the catalytic performance [15]. It was reported that DMSO could restrain the formation of undesirable products, such as condensation byproducts and HMF rehydration products, but increase the formation of furanose form over the selective dehydration of fructose [30]. However, in this work, the lower selectivity to furfural was obtained in DMSO over all of the catalysts except for H-mordenite (20) compared with the data obtained in water. An exceptionally low furfural selectivity was obtained over H-Y (5.1) in DMSO. This may be related to the fact that the furfural selectivity was very low in the absence of the catalyst in DMSO, as shown in Table 1. Homogeneous reactions, catalyzed by DMSO, can occur in the large cavities in H-Y (5.1). Therefore, the presence of large pores or cavities might not be desirable to obtain a high furfural selectivity in DMSO.

To investigate the effect of the amount of solid acid catalysts on the D-xylose dehydration, the reaction was carried out in the presence of different amounts of various selected catalysts-H- β (25), H-mordenite (20) and H-ferrierite (20)-in a different solvent system, as shown in Fig. 3. As usual, the D-xylose conversion increased with increasing amount of catalyst in all cases. On the other hand, no noticeable change in the furfural selectivity can be found with increasing amount of catalyst in the cases of H-ferrierite (20) in water, H- β (25) in water and H-mordenite (20) in DMSO. In the cases of H- β (25) in water/toluene, the furfural selectivity increased with increasing amount of catalyst, reached a certain value, and then leveled off. The lyxose selectivity decreased with increasing amount of catalyst, reached a certain value, and then leveled off in all cases except in the case of H-mordenite (20) in DMSO, where the lyxose selectivity increased with increasing amount of catalyst, reached a certain value, and then leveled off. The lyxose would be concurrently formed from the linear open chain of D-xylose through the acid-catalyzed hydrolysis of the hemiacetyl [2,20]. The lyxose can be converted into furfural through the dehydration steps [2,20].

The variation of the catalytic activity with the reaction time was monitored over H-mordenite (20) in DMSO and H- β (25) in water and water/toluene, as shown in Fig. 4. In all cases, the D-xylose conversion increased with increasing the reaction time. The furfural selectivity also increased initially, reached a certain value, and then leveled off. On the other hand, the lyxose selectivity decreased steeply with increasing the reaction time. It implies that the formation of the products such as furfural is more sensitive to the reaction

Table 2. The catalytic activity for the dehydration of D-xylose over the various solid acid catalysts in different solvent systems^a

Entry	Solvent	Catalysts	Amount of catalyst (g)	D-xylose conversion (%)	Furfural selectivity (%)	
1	Water	H-ferrierite (20)	1.00	62.6	24.5	
2		H- β (25)	0.40	61.3	36.9	
3		H-ZSM-5 (23)	0.30	56.8	30.2	
4		H-Y (5.1)	0.25	64.8	31.1	
5		H-mordenite (20)	0.55	59.0	26.1	
6		γ -Al ₂ O ₃	0.10	56.0	23.8	
7		Silica-alumina	0.40	57.0	26.2	
8	DMSO	H-ferrierite (20)	0.20	60.0	22.8	
9		H- β (25)	0.03	60.1	22.0	
10		H-ZSM-5 (23)	0.20	62.1	25.5	
11		H-Y (5.1)	0.30	61.1	1.6	
12		H-mordenite (20)	0.30	61.9	38.7	
13		γ -Al ₂ O ₃	0.03	60.8	18.4	
14		Silica-alumina	0.02	64.9	10.5	
15		W/T	H-ferrierite (20)	0.150	72.0	30.3
16			H- β (25)	0.150	66.1	37.4
17			H-ZSM-5 (23)	0.100	69.9	29.7
18			H-Y (5.1)	0.030	72.1	28.9
19			H-mordenite (20)	0.170	68.4	29.6
20			γ -Al ₂ O ₃	0.025	71.1	27.8
21			Silica-alumina	0.060	65.3	29.6

^aReaction conditions: D-xylose concentration=0.20 M, volume of solvent (Water, DMSO, and Water/toluene (3 : 7 by volume))=30 ml; reaction temperature=140 °C, reaction time=4 h

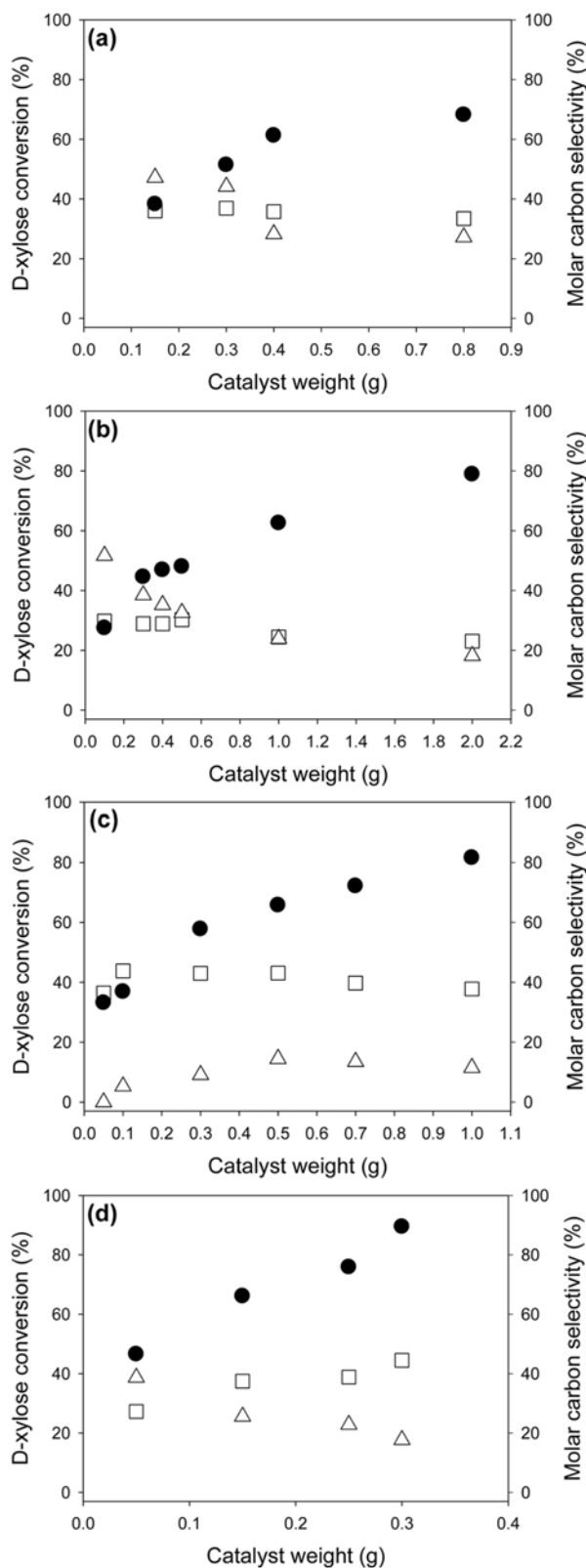


Fig. 3. D-xylose conversion (●) and molar carbon selectivity for the products such as furfural (□) and lyxose (△) over H-β(25) in water (a), H-ferrierite (20) in water (b), H-mordenite (20) in DMSO (c), and H-β(25) in water/toluene (v/v=3/7) (d). Reaction conditions: D-xylose concentration=0.20 M, volume of solvent=30 ml; reaction temperature=140 °C, reaction time=4 h.

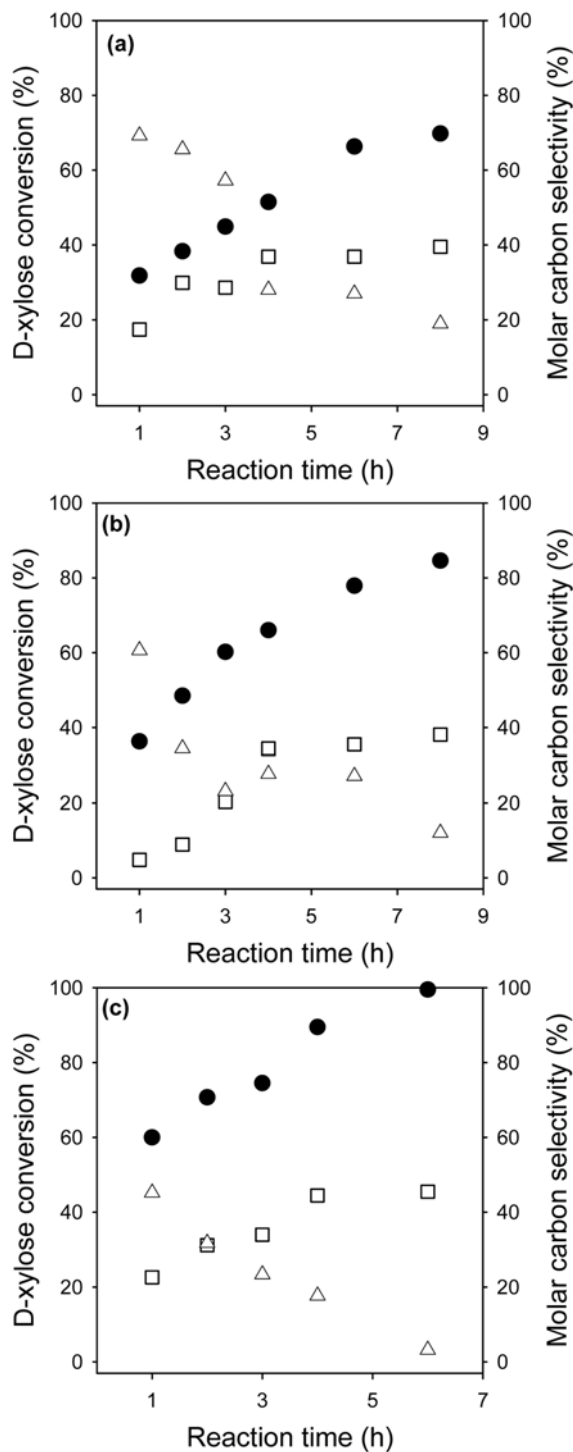


Fig. 4. Variation of D-xylose conversion (●) and molar carbon selectivity for the products such as furfural (□) and lyxose (△) with the reaction time over H-β(25) in water (a), H-mordenite (20) in DMSO (b) and H-β(25) in water/toluene (v/v=3/7) (c). Reaction conditions: D-xylose concentration=0.20 M, volume of solvent=30 ml; reaction temperature=140 °C, catalyst weight=0.30 g.

time than to the catalyst weight. O'Neill et al. examined the effect of the reaction time on the product distribution over H-ZSM-5 with a SiO₂/Al₂O₃ molar ratio of 14 in water. They reported that the isomer

of xylose (lyxose) was prominent in the initial stage and that organic acids and solid resin could be formed subsequently during the reaction [20]. The formation of solid resin was confirmed throughout in all experiments in this work, which is consistent with the results in the previous work [20].

CONCLUSIONS

The D-xylose conversion and furfural yield generally decreased with increasing SiO₂/Al₂O₃ molar ratio over the H-zeolites with the same crystal structure, irrespective of the kind of solvent system. This is closely related to the accessible acid sites. In the comparison study using three different solvent systems, the D-xylose conversion and furfural yield generally decreased in the following order: water/toluene>DMSO>water. In water and water/toluene, H-β(25) showed the highest furfural selectivity at a similar D-xylose conversion among the tested zeolites. On the other hand, H-mordenite (20) showed the highest furfural selectivity at a similar D-xylose conversion in DMSO.

ACKNOWLEDGEMENT

This work was supported by Priority Research Centers Program through the National Research Foundation of Korea (NRF) funded by the Ministry of Education, Science and Technology (2009-0094047). This work was also financially supported by a grant from the Industrial Source Technology Development Programs (10032003) of the Ministry of Knowledge Economy (MKE) of Korea.

REFERENCES

1. F. W. Lichtenthaler, *Carbohydr. Res.*, **313**, 69 (1998).
2. M. J. Antal, T. Leesomboon and W. S. Mok, *Carbohydr. Res.*, **217**, 71 (1991).
3. D. Montané, J. Salvadó, C. Torras and X. Farriol, *Biomass Bioenerg.*, **22**, 295 (2002).
4. R. Torget, P. Werdene, M. Himmel and K. Grohmann, *Appl. Biochem. Biotechnol.*, **24-25**, 115 (1990).
5. A. Demirbas, *Energy Source Part A*, **28**, 157 (2006).
6. B. P. Lavarack, G. J. Griffin and D. Rodman, *Biomass Bioenerg.*, **23**, 367 (2002).
7. T. Marzalletti, M. B. V. Olarte, C. Sievers, T. J. C. Hoskins, P. K. Agrawal and C. W. Jones, *Ind. Eng. Chem. Res.*, **47**, 7131 (2008).
8. W. Sangarunlert, P. Piumsomboon and S. Ngamprasertsith, *Korean J. Chem. Eng.*, **24**, 936 (2007).
9. M. Vázquez, M. Oliva, S. J. Téllez-Luis and J. A. Ramírez, *Biore-source Technol.*, **98**, 3053 (2007).
10. S. Lima, P. Neves, M. M. Antunes, M. Pillinger, N. Ignatyev and A. A. Valente, *Appl. Catal. A: Gen.*, **363**, 93 (2009).
11. A. S. Dias, M. Pillinger and A. A. Valente, *Appl. Catal. A: Gen.*, **285**, 126 (2005).
12. A. S. Dias, S. Lima, M. Pillinger and A. A. Valente, *Carbohydr. Res.*, **341**, 2946 (2006).
13. A. S. Dias, M. Pillinger and A. A. Valente, *Micropor. Mesopor. Mater.*, **94**, 214 (2006).
14. A. S. Dias, S. Lima, M. Pillinger and A. A. Valente, *Catal. Lett.*, **114**, 151 (2007).
15. A. S. Dias, M. Pillinger and A. A. Valente, *J. Catal.*, **229**, 414 (2005).
16. A. S. Dias, S. Lima, P. Brandão, M. Pillinger, J. Rocha and A. A. Valente, *Catal. Lett.*, **108**, 179 (2006).
17. A. S. Dias, S. Lima, D. Carriazo, V. Rives, M. Pillinger and A. A. Valente, *J. Catal.*, **244**, 230 (2006).
18. C. Moreau, R. Durand, D. Peyron, J. Duhamet and P. Rivalier, *Ind. Crop. Prod.*, **7**, 95 (1998).
19. S. Lima, M. Pillinger and A. A. Valente, *Catal. Commun.*, **9**, 2144 (2008).
20. R. O'Neill, M. N. Ahmad, L. Vanoye and F. Aiouache, *Ind. Eng. Chem. Res.*, **48**, 4300 (2009).
21. S. Lima, A. Fernandes, M. M. Antunes, M. Pillinger, F. Ribeiro and A. A. Valente, *Catal. Lett.*, **135**, 41 (2010).
22. A. Corma, *Chem. Rev.*, **95**, 559 (1995).
23. T. Barzetti, E. Selli, D. Moscotti and L. Forni, *J. Chem. Soc. Faraday Trans.*, **92**, 1401 (1996).
24. M. I. Zaki, M. A. Hasan, F. A. Al-Sagheer and L. Pasupulety, *Colloid. Surface A*, **190**, 261 (2001).
25. Y. T. Kim, K.-D. Jung and E. D. Park, *Appl. Catal. A: Gen.*, **393**, 275 (2011).
26. Y. T. Kim, K.-D. Jung and E. D. Park, *Micropor. Mesopor. Mater.*, **131**, 28 (2010).
27. C. A. Emeis, *J. Catal.*, **141**, 347 (1993).
28. S. A. Nolen, C. L. Liotta, C. A. Eckert and R. Gläser, *Green Chem.*, **5**, 663 (2003).
29. Q. Jing and X. Lü, *Chin. J. Chem. Eng.*, **15**, 666 (2007).
30. J. N. Chheda and J. A. Dumesic, *Catal. Today*, **123**, 59 (2007).